Paper No. 31

ISMS 2016

Numerical simulation of thermodynamic performance in a honeycomb ceramic channel

Bo Lan [a,b,]*, You-Rong Li [a]

[a] Key Laboratory of Low-Grade Energy Utilization Technologies and Systems of Ministry of Education, College of Power Engineering, Chongqing University, Chongqing, China, 400044
[b] China Coal Technology Engineering Group Chongqing Research Institute, Chongqing, China, 400037

ABSTRACT
In order to understand the thermodynamic performance in a honeycomb ceramic channel, a 3D numerical simulation was carried out using FLUENT. The effects of mass flow rate, solid heat capacity, and reversal time on temperature efficiency were investigated. Results show that with the increasing mass flow rate, the temperature efficiency decreases linearly and the pressure drop increases linearly in each half-cycle. For computed cases the effect of solid heat capacity on the temperature efficiency is negligible. With the increasing reversal time, the temperature efficiency decreases slowly in the bed heated period, and is not influenced in the bed cooled period.
KEYWORDS: numerical simulation; honeycomb ceramic channel; thermodynamic performance; temperature efficiency

1. INTRODUCTION

Methane (CH_4) is a greenhouse gas (GHG) that is 21 times more potent than carbon dioxide (CO_2) in terms of trapping heat in the atmosphere over a timeframe of 100 years (Gosiewski et al., 2008). Ventilation air methane (VAM) emitted from underground coal mines constitutes a major part of greenhouse gas emissions from coal mining and is a wasted resource. The utilization methods of VAM have been studied extensively in recent years (Su et al., 2005; Su et al., 2006; Yin et al., 2010; Karacan et al., 2011; Baris, 2013; Krzysztof et al., 2014; Martinez et al., 2014; Zhang et al., 2014).

The utilization methods can be divide into ancillary use and principle use (Su et al., 2005). For the ancillary use, VAM is used to substitute ambient air in combustion processes, including gas turbines, internal combustion engines, and coal-fired power stations. For the principle use, the methane in VAM is used as a primary energy source.

Nowadays, only the thermal flow-reversal reactor (TFRR) and catalytic flow-reversal reactor (CFRR) are seriously taken into account for industrial usage. The only difference between these two devices is with respect to the use of catalyst. Honeycomb ceramic is the most important component of TFRR and CFRR. However, the thermodynamic characteristics of honeycomb ceramic channel have not been clearly studied.

The aim of this study is to investigate the temperature migration rule in honeycomb ceramic beds, and examine the effects of mass flow rate, solid heat capacity, and reversal time on temperature efficiency.

2. PHYSICAL AND MATHEMATICAL MODEL

2.1 Physical model

There are millions of honeycomb ceramic channels in a regenerative oxidation bed. The flow and thermal performance of each honeycomb ceramic channel is similar to the others.

The geometry of a single honeycomb ceramic channel and the coordinate system is shown in Figure 1. The channel size is 3 mm × 3 mm and the wall thickness is 0.7 mm. The length is 300 mm.

One heat exchange cycle is comprised of two flow reversals, so each flow reversal is a half-cycle. During the first half-cycle, hot gas enters from the right and leaves through the left. The bed is heated and the fluid is cooled down. This half-cycle is called the bed heated period. After a time interval the flow direction is reversed. Cold VAM enters from the left and leaves through the right. The bed is cooled down and the VAM is heated. This half-cycle is called the bed cooled period.

* Corresponding author – email: lbmky@163.com

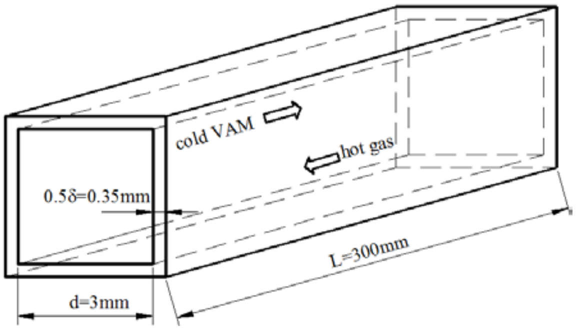

Figure 1: Physical model.

2.2 Governing equations

The honeycomb ceramic channel has a three-dimensional unsteady flow. There are three different heat transfer processes: heat conduction process inside the fluid, heat convection between the solid and fluid, and heat conduction inside the solid.

The following assumptions are introduced in the present model: (1) radiative heat transfer is neglected because air, oxygen, and nitrogen are not able to emit and absorb radiation energy; (2) the heat dissipation on the outer wall of the channel is neglected; (3) the air physical parameters are applied for VAM and hot fluid; (4) methane oxidation generally occurs in the combustion chamber, rather than in the honeycomb ceramic channel, and this paper focuses on the heat transfer law in the honeycomb ceramic channel, ignoring the effect of methane oxidation.

With the above assumptions, the governing equations of flow and heat transfer could be expressed as follows:

Continuity equation

$$\frac{\partial \rho}{\partial t}+\nabla\cdot(\rho U)=0 \tag{1}$$

where ρ , t , U are the fluid density, time, velocity, respectively.

Momentum equation

$$\frac{\partial(\rho U)}{\partial t}+U\cdot\nabla(\rho U)=-\nabla p+\mu\nabla^2 U+S \tag{2}$$

where p , μ , S are pressure, the fluid dynamic viscosity, source term, respectively.

Fluid energy equation

$$\frac{\partial(\rho T)}{\partial t}+\nabla\cdot(\rho UT)=\nabla\cdot\left(\frac{\lambda}{c_p}\nabla T\right)+\varPhi \tag{3}$$

where T , λ , c_p , $\varPhi$ are temprature, the fluid conductivity, the fluid specific heat, dissipative function, respectively.

State equation

$$p=\rho R_g T \tag{4}$$

where R_g is the gas constant.

Solid energy equation

$$\frac{\partial(\rho_s T)}{\partial t}=\nabla\cdot\left(\frac{\lambda_s}{c_{ps}}\nabla T\right) \tag{5}$$

where ρ_s , λ_s , c_{ps} are the solid density, conductivity, specific heat, respectively.

2.3 Physical parameters of fluid and solid

The physical parameters of fluid are listed in Table 1.

Table 1 :The physical parameters of fluid.

Items	Unit	Value			
		273 K	473 K	773 K	1173 K
ρ	kg/m^3	1.293	0.746	0.456	0.301
C_p	J/(kg·K)	1005	1026	1093	1172
λ	10^{-2}W/(m·K)	2.44	3.93	5.74	7.63
μ	10^{-6}kg/(m·K)	16.7	26	36.2	46.7

The physical parameters of solid are defined as follows:

$$\rho_s=2500 \qquad \mathrm{kg/m^3} \tag{6}$$

$$\lambda_s=0.000666T+1.305 \qquad \mathrm{W/(m\cdot K)} \tag{7}$$

$$C_{ps}=0.23T+C_{ps0} \qquad \mathrm{J/(kg\cdot K)} \tag{8}$$

where C_{ps0} is a parameter determined by the solid material.

2.4 Boundary conditions

A symmetrical boundary condition is applied for the outer walls of the honeycomb ceramic (x=0mm, x=3.7mm, y=0mm, y=3.7mm), and adiabatic boundary condition for the front and back wall (z=0mm, z=300mm). A coupled boundary condition is used for the inner walls of the honeycomb ceramic channel.

Mass-flow-inlet boundary condition is applied for the inlet, and pressure-outlet boundary condition for the outlet. The inlet temperatures of hot and cold fluid are constant and equal to 1173 K and 293 K, respectively.

2.5 Numerical methods

The model is solved by FLUNET. The governing equations are discretized by the finite difference method. The central difference approximation is applied for the diffusion terms and the second order of upwind scheme is used for the convection terms.

The SIMPLEC algorithm is applied to couple the pressure and velocity variables.

In order to check the validation of this model, a simulation is carried out under the same conditions with the case carried out by (Zhang et al., 2010). In the case, The channel size is 3 mm × 3 mm, the wall thickness is 1 mm, and the length is 100 mm. The obtained pressure drop is 15.7 Pa with inlet velocity of 2 m/s, which is comparabe with the result of 15 Pa carried out by Zhang (2010).

3. RESULTS AND DISCUSSION

A 3D numerical simulation is carried out to investigate the thermodynamic performance by varying mass flow rate, solid heat capacity, and reversal time. In this work seven cases are computed, as shown in Table 2. The mass flow rate and reversal time are represented as Q_m and t_r, respectively.

Table 2: The seven cases (A-G) computed in this work.

Items	Unit	A	B	C	D	E	F	G
C_{ps0}	J/kg·K	907	907	907	750	1050	907	907
Q_m	kg/s	1×10^{-5}	1.5×10^{-5}	2×10^{-5}	1×10^{-5}	1×10^{-5}	1×10^{-5}	1×10^{-5}
t_r	s	30	30	30	30	30	15	45

3.1 Thermodynamic performance in the honeycomb ceramic channel

In the bed heated period the hot fluid temperature (T_h) is higher than the solid temperature (T_s), and heat transfers from the hot fluid to the solid. As time goes by, the solid temperature increases gradually. The solid temperature profile along the flow direction moves upward, as shown in Figure 2. It leads to a reduction of the temperature difference between the fluid and solid. The heat storage capacity of the solid reduces and the fluid outlet temperature increases. As a result, the fluid temperature distribution moves upward over time. The temperature change rates of the hot fluid and solid are -1.83 K/s and 2.14 K/s, respectively.

In the bed cooled period the rules are reversed. Due to the lower cold fluid temperature (T_c), heat transfers from the solid to the fluid. The temperature distribution of the cold fluid and solid along the flow direction moves down over time, as shown in Figure 3. The temperature change rates of the cold fluid and solid are 1.77 K/s and -2.12 K/s, respectively.

Logarithmic mean temperature differences between the fluid and solid decrease over time in each half-cycle, as shown in Figure 4. Meanwhile the heat flux on the inner walls of the channel decreases linearly, and the heat transfer capability deteriorates, as shown in Figure 5.

3.2 Effect of mass flow rate

In order to evaluate the heat exchange performance of the honeycomb ceramic channel, the temperature efficiency is defined as follows:

The temperature efficiency in bed heated period

$$\varepsilon_h = \frac{T_{h,i} - \overline{T}_{h,o}}{T_{h,i} - T_{c,i}} \tag{9}$$

where $T_{h,i}$ and $\overline{T}_{h,o}$ are the inlet and average outlet temperatures of the hot fluid, respectively, and $T_{c,i}$ is the inlet temperature of the cold fluid.

The temperature efficiency in bed cooled period

$$\varepsilon_c = \frac{\overline{T}_{c,o} - T_{c,i}}{T_{h,i} - T_{c,i}} \tag{10}$$

where $\overline{T}_{c,o}$ is the average outlet temperature of the cold fluid.

Figure 6 shows the effect of mass flow rate on the temperature efficiency. In the bed heated period, the temperature efficiency decreases linearly with the increase in mass flow rate. The reason is that more heat is intaken by a higher mass flow rate, and the solid cannot fully absorb the increasing heat, and more heat is carried out by the hot fluid. In the bed cooled period, the temperature efficiency also decreases with the increasing mass flow rate.

Figure 7 shows that the pressure drops are increasing with the increase in mass flow rate in each half-cycle. With the same mass flow rate, the pressure drop in the bed heated period is higher than that in the bed cooled period.

The above results indicate that reducing mass flow rate is positive for improving temperature efficiency and reducing pressure drop.

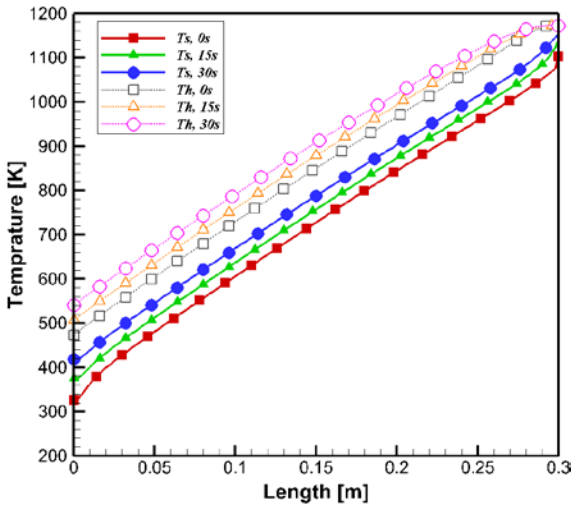

Figure 2: Temperature distributions of the hot fluid and solid along flow direction in bed heated period for case A.

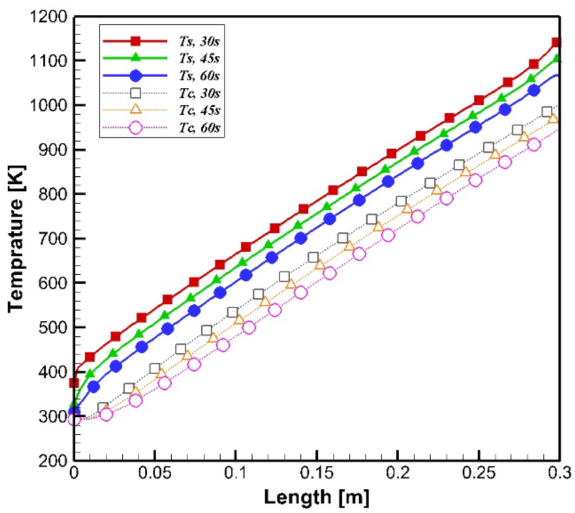

Figure 3: Temperature distributions of the cold fluid and solid along flow direction in bed cooled period for case A.

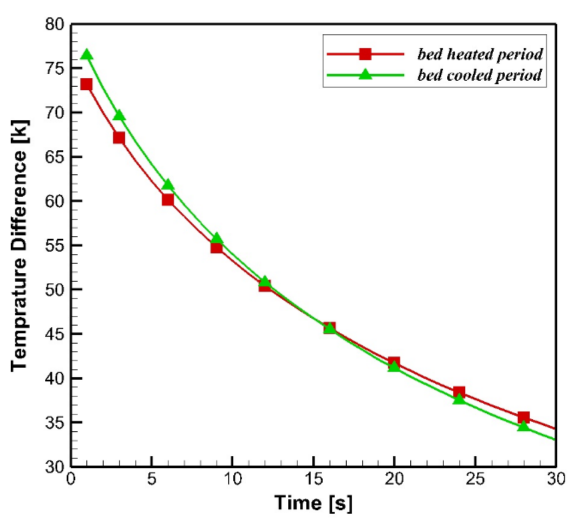

Figure 4 :Variation of logarithmic mean temperature difference between the fluid and solid in one heat exchange cycle for case A

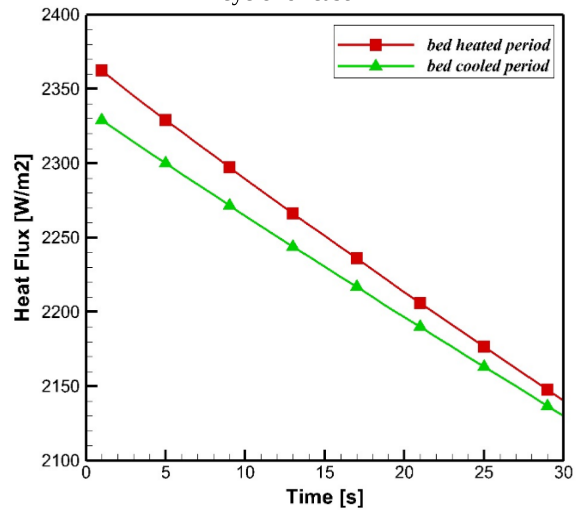

Figure 5: Variation of heat flux in one heat exchange cycle for case A.

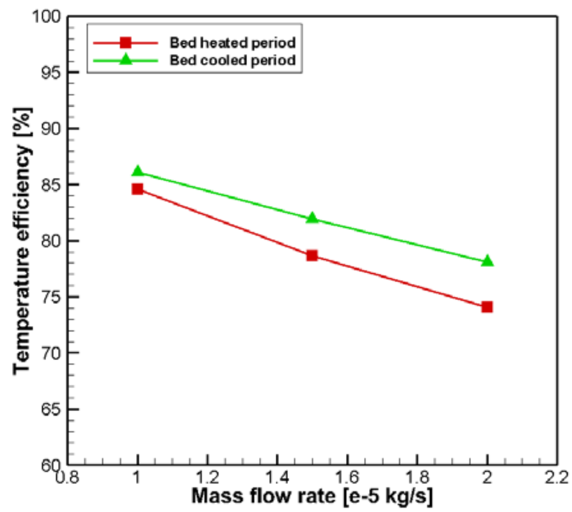

Figure 6: Effect of mass flow rate on the temperature efficiency.

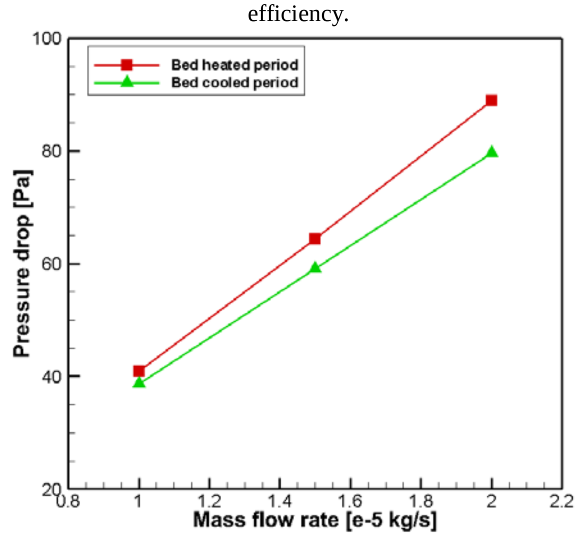

Figure 7: Effect of mass flow rate on pressure drop.

3.3 Effect of solid heat capacity

Figure 8 shows that the larger the specific heat is, the more significant the variation of outlet temperature in each half-cycle. However the variation of average outlet temperatures is small for both hot and cold fluid in three computed cases.

As shown in Figure 9, in the bed heated period the temperature efficiency is almost not influenced by heat capacity, and in the bed cooled period the temperature efficiency increases slowly with the increasing heat capacity.

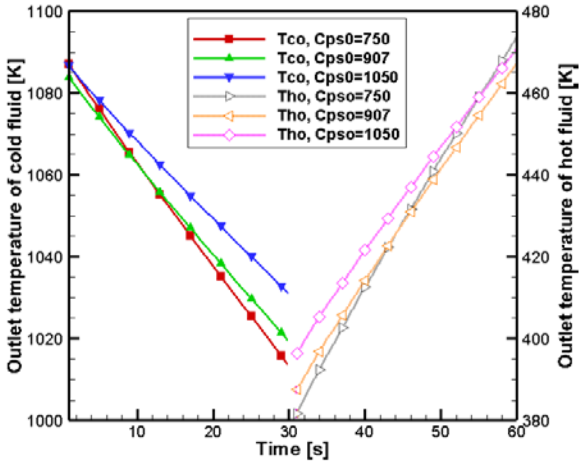

Figure 8: Outlet temperatures of hot and cold fluid in one heat exchange cycle ($T_{h,o}$: hot fluid, $T_{c,o}$: cold fluid).

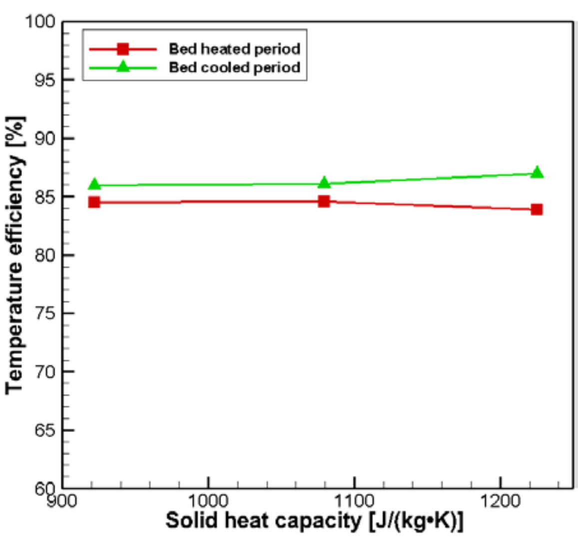

Figure 9: Effect of solid heat capacity on the temperature efficiency.

3.4 Effect of reversal time

Figure 10 shows the effect of reversal time on the temperature efficiency. In the bed heated period, the temperature efficiency decreases slowly with the increasing reversal time. In the bed cooled period, the temperature efficiency is almost not influenced by reversal time.

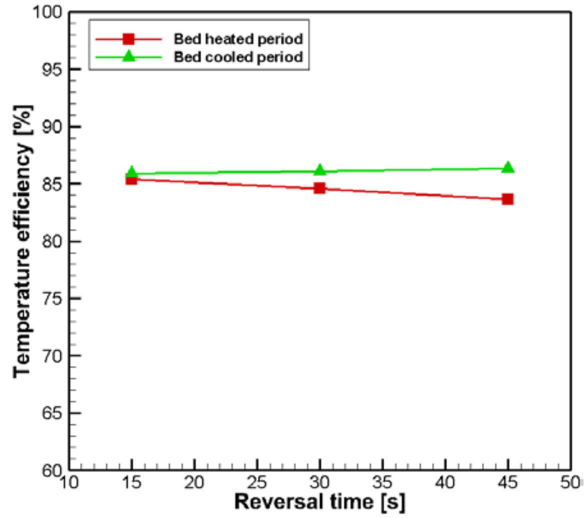

Figure 10: Effect of the reversal time on the temperature efficiency

4. CONCLUSION

A 3D numerical simulation was performed to investigate the thermodynamic performance in honeycomb ceramic channel. The following conclusions were made:

1) In the bed heated period the temperature change rates of the hot fluid and solid are -1.83 K/s and 2.14 K/s, respectively. In the bed cooled period the change rates of the cold fluid and solid are 1.77 K/s and -2.12 K/s, respectively. Logarithmic mean temperature differences between the fluid and solid decreased over time in each half-cycle, and the heat flux on the inner walls of the channel decreased linearly.

2) With the increasing mass flow rate, the temperature efficiency decreased linearly, and the pressure drop increased linearly in each half-cycle.

3) For computed cases the effect of solid heat capacity on the temperature efficiency is ignorable.

4) With the increasing reversal time, the temperature efficiency decreased slowly in the bed heated period, and was almost not influenced in the bed cooled period.

5. ACKNOWLEDGEMENT

This work is supported by National Science and Technology Major Project (Project Number 2011ZX05041-005).

6. REFERENCES

Baris K. (2013). Assessing ventilation air methane (VAM) mitigation and utilization opportunities: A case study at Kozlu Mine, Turkey.

Energy for Sustainable Development, Volume 17, pp. 13-23.

Gosiewski K., Matros Y.S., Warmuzinski K., Jaschik M., and Tanczyk M. (2008). Homogeneous vs. catalytic combustion of lean methane—air mixtures in reverse-flow reactors Chemical Engineering Science, Volume 63, pp. 5010-5019.

Gosiewski, K., and Pawlaczyk, A. (2014). Catalytic or thermal reversed flow combustion of coal mine ventilation air methane: What is better choice and when. Chemical Engineering Journal, Volume 238, pp. 78-85.

Martinez D.M., Cluff D.L., and Jiang X. (2014). Numerical investigation of the burning characteristics of ventilation air methane in a combustion based mitigation system. Fuel, Volume 133, pp. 182-193.

Karacan C.O., Ruiz F.A., Cote M., and Phipps S. (2011). Coal mine methane: A review of capture and utilization practices with benefits to mining safety and to greenhouse gas reduction. International Journal of Coal Geology, Volume 88, pp. 121-156.

Karakurt I., Aydin G., and Aydiner K. (2011). Mine ventilation air methane as a sustainable energy source . Renewable and Sustainable Energy Reviews, Volume 15, pp. 1042-1049.

Su, S., Beath, A., Guo, H., and Mallett, C. (2005). An assessment of mine methane mitigation and utilization technologies. Progress in Energy and Combustion Science, Volume 31, pp. 123-170.

Su S., and Agnew J. (2006). Catalytic combustion of coal mine ventilation air methane. Fuel, Volume 85, pp. 1201-1210.

Yin J., Su S., Yu X.X., and Weng Y.W. (2010). Thermodynamic characteristics of a low concentration methane catalytic combustion gas turbine. Applied Energy, Volume 87, pp. 2102-2108.

Zhang Y.X., Doroodchi E., and Moghtaderi B. (2014). Utilization of ventilation air methane as an oxidizing agent in chemical looping combustion. Energy Conversion and Management, Volume 85, pp. 839-847.

Zhang Z.X., Liu Y.Q., Gao Z.Q., and Liu R.X.(2010). Simulation study of flow and heat transfer in ceramic regenerator. ICE&Powerplant, Volume 116, pp. 18-22.